Composite Structures 158 (2016) 20–29

Contents lists available at ScienceDirect

Composite Structures

journal homepage: www.elsevier.com/locate/compstruct

The electrically conductive carbon nanotube (CNT)/cement composites for accelerated curing and thermal cracking reduction

G.M. Kim [a], B.J. Yang [b,*], G.U. Ryu [a], H.K. Lee [a]

[a] Department of Civil and Environmental Engineering, Korea Advanced Institute of Science and Technology (KAIST), Daehak-ro 291, Yuseong-gu, Daejeon 34141, Republic of Korea
[b] Multifunctional Structural Composite Research Center, Institute of Advanced Composite Materials, Korea Institute of Science and Technology (KIST), Chudong-ro 92, Bongdong-eup, Wanju-gun, Jeonbuk 55324, Republic of Korea

ARTICLE INFO

Article history:
Received 17 March 2016
Revised 5 September 2016
Accepted 9 September 2016
Available online 10 September 2016

Keywords:
Joule heating characteristics
Carbon nanotube
Cementitious composites
Accelerated curing
Thermal analysis

ABSTRACT

A functional cementitious composite for smart structures has attracted much attention due to their potential possibilities of application. In this paper, the accelerated curing and thermal cracking reduction with carbon nanotube (CNT)/cement composites are studied experimentally and theoretically. The heating element was fabricated by incorporation CNT into cement, and the cementitious composite block was placed in the middle of mortar samples. In order to generate and evaluate the heating performance, copper wires connected to the composite block were extended to a DC power supply. The variations of material characteristics including curing, thermal, electrical and mechanical properties of both the composite block and the sample were investigated. The experimental test results showed that the proposed curing was capable of improving the compressive strength by 40% at 24 h. In addition, based on the experimentally obtained material constants, a series of thermal analysis of mitigation level of thermal crack in larger scale were carried out. The electrically conductive CNT/cement composite block was found to be applicable to the cement mortar curing and reduction of thermal cracking of massive concretes structures.

1. Introduction

The strength development of concrete is dictated by the hydration reaction of the cement, which is influenced by curing conditions such as the temperature and humidity during the early stage of curing [25]. The curing condition is therefore responsible for the development of phases in concrete which can resist external force, preventing the formation of cracks to develop sufficient strength and ultimately enhancing the durability [1,38]. In particular, the hydration reaction at an early age is highly dependent on the temperature [16]. This implies that an increase in the curing temperature increases the rate of the hydration reaction, enhances the development of strength and ultimately reduces the construction period [32]. Early strength development in concrete by various accelerated curing methods has been a subject of numerous studies [30,34,45,21].

Steam curing and autoclave methods are the most conventional techniques in the construction practice [30,34]. These methods, however, strongly rely on the conduction of heat from the exterior [27]; therefore, the heat flux is distributed non-uniformly [17]. In addition, these approaches require the use of expensive equipment [17,28]. Xuenquan et al. [45] and Leung and Pheeraphan [27] proposed the use of microwave energy for the curing of cementitious materials. Compared to conventional techniques, the curing period of the microwave method is much shorter than in the steam curing and autoclave methods [45]. However, as with the steam curing method, a specially manufactured expensive mold, consisting of microwave equipment, should be applied to the system [27,42].

Electrical curing is the most advanced accelerated curing technique among all others, providing ease of construction. Its effects are evidenced in various experimental studies [43]. Meanwhile, this method utilizes the internal water in the concrete in a fresh state, for which the electrical resistivity is reduced to as low as 5000 Ω·cm, and it inevitably requires a power supply of more than 500 W, as reported in Wilson and Gupta [43] in case that the size of specimen is 150 mm × 150 mm × 150 mm. Additionally, the electrical resistivity dramatically increases as the internal water evaporates [43], and debonding is unavoidable at the interface between the electric coils and the cement paste, where the heat is transferred [12], indicating that the expected performance does not greatly exceed those by existing technologies and that the application of this method for mass concrete remains challenging [21].

Metallic electrical conductivity and the high aspect ratio of CNT were shown to be capable of creating a conductive pathway within a cementitious composite incorporating less than 1.0 wt% of CNT

* Corresponding author.
E-mail address: bj.yang@kist.re.kr (B.J. Yang).

http://dx.doi.org/10.1016/j.compstruct.2016.09.014
0263-8223/

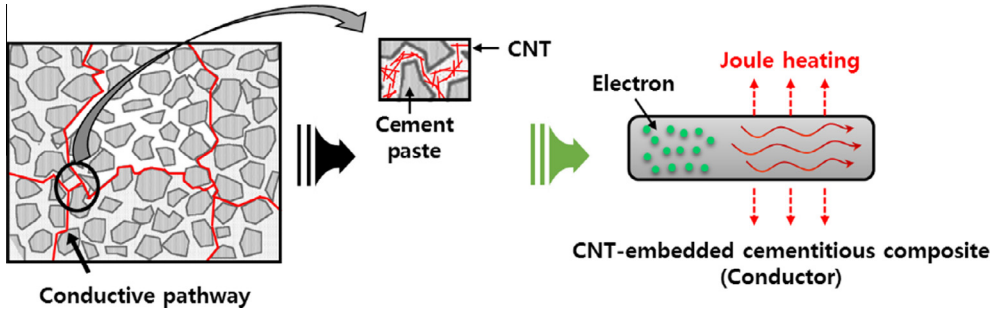

Fig. 1. A schematic description of the Joule heating mechanism.

and increasing the electrical conductivity of the composite by a factor of 10^4–10^5 [49]. Applying voltage to the composite with inherited high electrical conductivity results in Joule heating by the flow of electrons through the electrical conductive network, as shown in Fig. 1 [42]. The heat generated by Joule heating can be expressed as Eq. (1) [42,5],

$$Q = \frac{V^2 t}{R} \tag{1}$$

where Q denotes the heat generated by the input voltage (V) during time (t) and R denotes the electrical resistance of the conductor (e.g., the CNT/cement composite block) [5]. It is evident from Eq. (1) that lower electrical resistance of the composite leads to greater generation of heat. That is, lower electrical resistivity, which is proportional to the electrical resistance, leads to more efficient heat generation [23]. The detailed heating characteristics of CNT/cement composite block were investigated in a recent study conducted by Kim et al. [23].

In the present study, an accelerated curing of cement mortar with electrically conductive CNT/cement composite block is proposed. An electrically conductive CNT/cement composite block was placed in the middle of cement mortar samples. Copper wires connected to the composite block were extended to a DC power supply. The heating and electrical characteristics of the composite block and the specimen, and the compressive strength of the specimen were investigated. In addition, mitigation level of thermal crack in concrete with the CNT-embedded cementitious composites is numerically investigated. Based on the experimentally obtained material constants, a series of thermal analysis were carried out.

2. Experimental program

2.1. Sample preparation

Heating characteristics of CNT/cement composite block reported by the authors are briefly recapitulated below. The CNT/cement composite block with the CNT content of more than 0.3% had significantly reduced electrical resistivity, exceeding the percolation threshold for the creation of an electrical conductive pathway and the composites with the CNT content of 2.0% reached a temperature of 70 °C within 30 min [23]. The influence of a cyclic heating on the heat-dependent mechanical characteristics of the composites was also addressed by measuring the compressive strength of a sample [23]. The composite with a CNT content of 0.6% below experienced an increase in the compressive strength by 30% due to additional hydration, while that with the CNT content of 1.0% above experienced damage to the matrix during the cyclic heating process [23]. Consequently, composites with the CNT content of 0.6% have shown the most outstanding durability in terms of the heating performance. CNT/cement composite blocks with the CNT content of 0.6% were thus prepared for accelerated curing of cement mortar in this study.

Type 1 Portland cement and silica fume were used as a binder. The spherical particles of silica fume are capable of enhancing the dispersion of CNT by penetrating into the CNT agglomerates and reducing the van der Waals force [46,19]. The silica fume used was a proprietary product of Elkem Inc. (EMS-970), with an average diameter greater than 5 μm. The Poly-carboxylic acid based superplasticizer (GLENIUM 8008 made by BASF Pozzolith Ltd.) used here served to control the workability and to improve the dispersion of the CNT particles in the cement matrix [24]. In a previous study conducted by the authors, a lower water content in the composite was found to yield higher continuity in the CNT particles, thus enhancing the conductive pathways [23]. That is, the use of water is to be minimized while the workability is to be achieved via the dominant use of a superplasticizer. The multi-walled carbon nanotubes with a purity level of 95% were a proprietary product of Hyosung Inc. Korea, and were produced by the thermal chemical vapor deposition (CVD) growth method [13]. The length and diameter of the CNT were approximately 10 μm and 12–40 nm, respectively [47].

A CNT/cement composite block was produced on the basis of the previous study conducted by the authors [23]. It had a CNT content of 0.6% by weight of the cement. The mix proportion and geometry of the composite block are given in Table 1 and Fig. 2 (a), respectively. The dimensions of the composite block were 25 mm × 25 mm × 25 mm. Silver paste (Nanonix Inc., Korea) was applied onto two copper electrodes prior to inserting into the composite block as means to enhance the contact between the cement paste and the electrodes [41,40,33]. The height and width of the electrodes were 45 mm and 10 mm, respectively. The electrodes were inserted into the composite block at an interval of 10 mm. The details regarding the mixing procedure can be found in Kim et al. [23].

The mix proportion and the geometry of a cement mortar sample in which the composite block was placed for the proposed curing are shown in Table 2 and Fig. 2(b), respectively. The cement mortar sample was a mortar with the w/c of 0.4. The specific gravity of the sand used in the mortar was 2.5. The dimensions of the cement mortar sample were 100 mm × 200 mm, conforming to ASTM C39 [4]. The fabrication procedure was as follows: Cement, water and aggregate were stirred in a Hobart mixer for 5 min. The mixture was poured into a cylindrical mold until half of the mold was filled. The mold was then tamped with a tamping rod. The electrodes inserted into the composite block were welded with copper wires connected to a DC power supply. The composite block was placed into the center of the cylinder and the mold was completely filled with the mortar mixture, ensuring that the two wires remain contactless (see Fig. 2(b)). Finally, the sample was wrapped and cured at 25 ± 5 °C for the designated number of hours.

Table 1
Mix proportion of CNT/cement composite block.

Sample	Cement	CNT	Silica Fume	Water	Superplasticizer	Target flow (mm)
CNT_0.6	100	0.6	10	28	2.0	110 ± 5

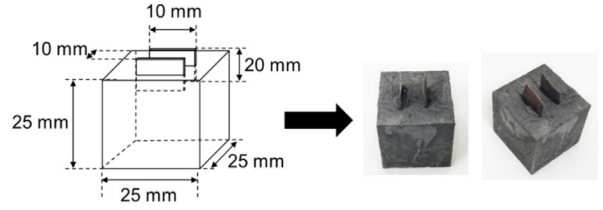

(a) CNT/cement composite block

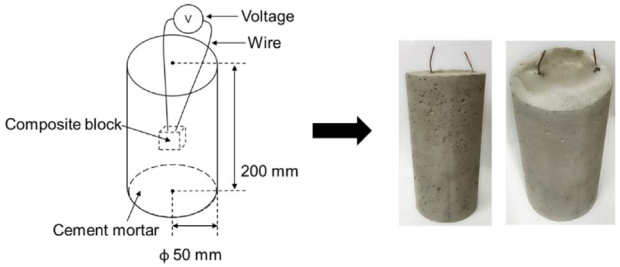

(b) Cylindrical mortar sample with the composite block

Fig. 2. Geometry of the samples used in experiment: (a) the CNT/cement composite block and (b) the cylindrical mortar sample with the composite block.

Table 2
Mix proportion of cylindrical mortar sample.

Mix proportions (specific gravity)		
Cement	Fine aggregates	Water
2700 (3.10)	5400 (2.5)	1070 (1.0)

2.2. Test methods

The electrical resistance values of the composite blocks were measured by means of the two-probe method using a portable digital multimeter (Agilent Technologies, U1242A) and recorded manually. The electrical resistivity was obtained by converting the electrical resistance values recorded by a digital multimeter, as in previous works [26,14,37]

$$\rho = R\frac{A}{L} \tag{2}$$

where ρ denotes the electrical resistivity (Ω·cm), R is the electrical resistance (Ω), A is the cross-sectional area of the samples in contact with the electrodes (cm^2), and L represents the distance between the electrodes (cm) [26,6].

The current of the composite block was measured prior and subsequent to the insertion into the cement mortar sample. A DC power supply (PL-3005S) capable of applying input voltage by 30 V was used to provide input power to the composite block and the composite block placed in the cement mortar samples, and their electrical current values over the time were recorded manually [36,39]. In addition, a K-type thermocouple was attached onto the surface of the composite block and the cement mortar samples, and was linked to a data logger (Agilent Technologies, 34972A) to record the surface temperature values. The cement mortar sample with the embedded composite block was placed in a commercial Styrofoam box to prevent the temperature from decreasing by the diffusion of heat during the proposed curing. In order to analyze a change in the microstructure of the composite block induced by the proposed curing, the scanning electron microscope (SEM) analysis was carried out by using Magellan 400 (FEI Co.). The specimens were immersed in acetone and then desiccated for 48 h to arrest hydration and to remove internal water in the composite [24]. In addition, the heat diffusion from the composite block and through the cement mortar sample was characterized using a thermo-graphic camera (VarioCam®hr, InfraTec). The camera was set 25 cm away from the target sample, and the sampling rate of the camera was set to 0.5 Hz.

Table 3
Electrical resistivity of CNT/cement composite block.

Sample	Electrical resistivity(Ω·cm)	
	Air dry	Oven dry
CNT 0.6%	543.72(174.3)	560(175.52)

*Values in parentheses are standard deviations.

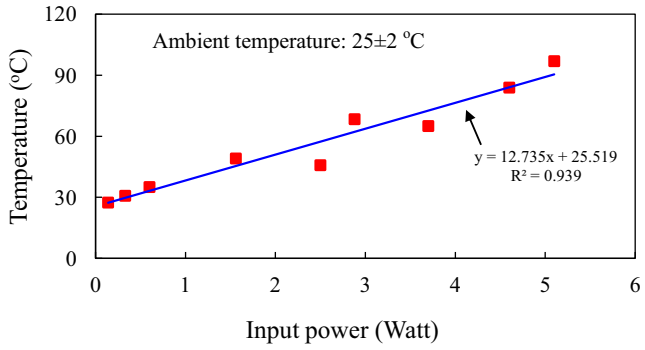

(a)

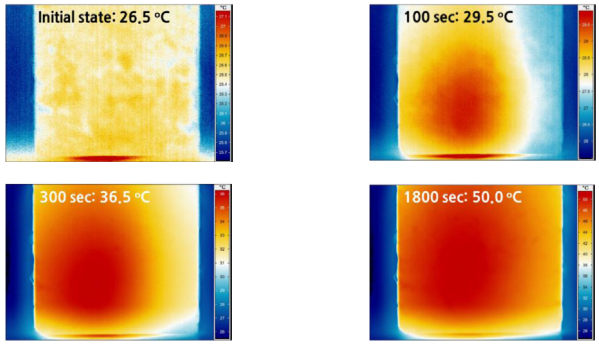

(b)

Fig. 3. (a) Temperature increase in the composite block with varying input power and (b) thermo-graphic images of composite block at a fixed input power (5 W) at different time instants (Supplementary video material of Fig. 3 will be available in the online version of the paper).

The cement mortar sample was demolded and the copper wires were cut prior to a compressive strength test. The top surface of the samples was ground to prevent concentrated loading during the compressive strength test. The compressive strength test was conducted in accordance with ASTM C39 [4]. A universal testing machine (UTM) with a load cell of 3,000 kN was used for the test. The displacement rate was fixed at 0.02 mm/s. Three samples were tested, and the average values were calculated.

3. Heat generation and electrical characteristics of the CNT/cement composite block

3.1. Heat generation characteristics of the composite block

A total of six CNT/cement composite blocks with CNT of 0.6 wt% were produced in the present study. Their electrical resistance values are shown in Table 3. The average air-dried and oven-dried electrical resistance level were almost similar. Kim et al. [23] stated that a CNT/cement composite block with a CNT content below the percolation threshold experiences reduction in the continuity among CNT particles and increase in the electrical resistivity due to internal water evaporation [23]. That is, the conductive pathway in the composite was continuous and the electrical resistivity of the composite block was unaffected by the evaporation of the internal water.

The surface temperature of the composite block as a function of the input power is shown in Fig. 3(a), showing a linear relationship. As evidenced in the previous study conducted by the present authors, control of the input power is an effective means of controlling the temperature [23]. However, it is also reported in our previous study that the electrical resistivity of CNT/cement composite increased during heating [23]. Therefore, the input voltage applied to the composite block in the present study was varied to ensure a constant input power. A thermal infrared image of the surface of the composite block supplied with an input power of 5 W is shown in Fig. 3(b). The temperature diffusion of the composite block became nearly saturated to the surface within 30 min.

3.2. Heat generation and electrical characteristics of the composite block placed in cylindrical mortar specimen

A general form of temperature curve for electrical curing reported in previous studies is shown in Fig. 4(a) [43]. The curve is divided into four regions as follows: (a) the first region is before the supply of input power and is termed as a setting period in which a sample is cured under ambient conditions. (b) The second region is a heating period where the temperature begins to increase as the input power is supplied. (c) The third region is an isothermal period where the increased temperature is maintained, and (d) the fourth region is the last phase of the curing regime and is termed a natural cooling period where the temperature gradually decreases.

The temperature curve of a composite block placed in a cement mortar sample is shown in Fig. 4(b). It should be noted that while all regions are denoted, the setting period is excluded from the figure. The setting period determines whether the matrix of a cementitious material can resist the thermal stress developed during the course of the curing. Accordingly, the setting period was varied; the P-1 sample denotes a cement mortar sample with a setting period of 1 h, while the P-6 sample denotes that with 6 h. The temperature curve of the P-1 and P-6 samples were similar in terms of the

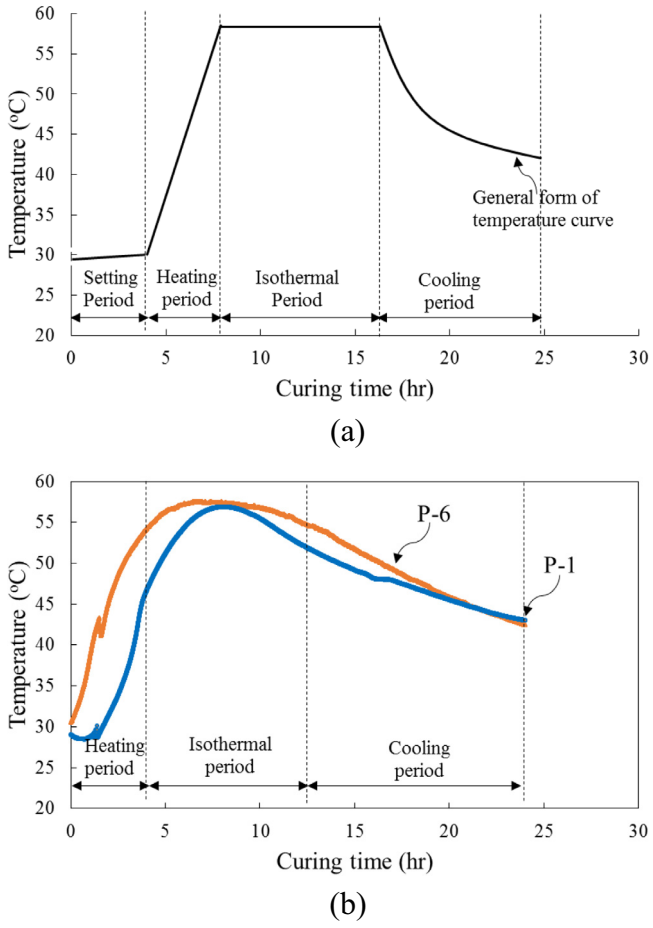

Fig. 4. (a) General form of temperature curve for electrical curing in previous studies [43] and (b) Temperature curve of mortar samples with composite block.

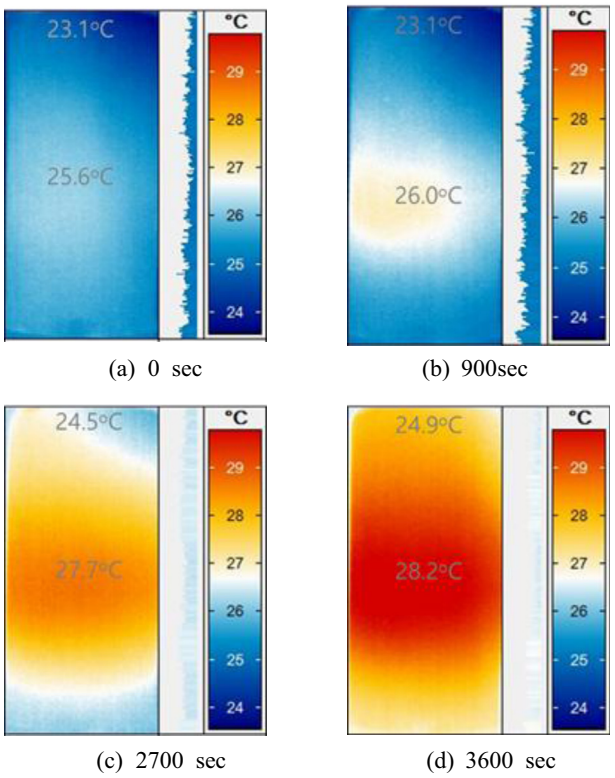

Fig. 5. Thermo-graphic images of P-6 sample at 5 W after (a) 0 s, (b) 15 min, (c) 45 min, and (d) 60 min.

shape with the general form of a temperature curve, as shown in Fig. 4(b). A temperature increase was observed for a period of 4 h immediately after the supply of input power and an isothermal period was thereafter observed until 12.5 h. Lastly, a cooling period was observed, during which the temperature gradually decreased.

A thermo-graphic image of the P-6 sample in which a composite block was placed in the mid-plane and supplied with an input power of 5 W as a function of time, is shown in Fig. 5. It was noted that the temperature increased from the center of the sample where the composite block was located. Furthermore, the heat diffused toward the surface and the temperature of the entire sample increased. That is, the heat diffusion from the composite block was appropriate such that it reached the outer surface of the sample.

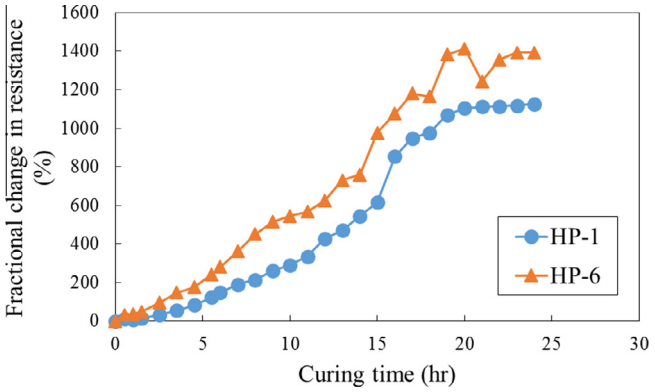

Fig. 6. Fractional change in electrical resistance of composite blocks placed in mortar sample.

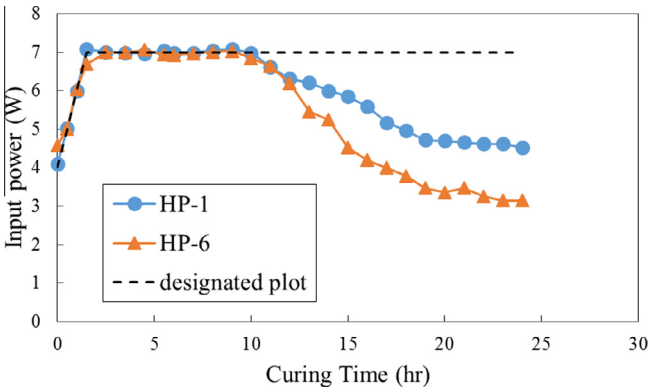

Fig. 8. Input power applied to composite block for curing of mortar sample.

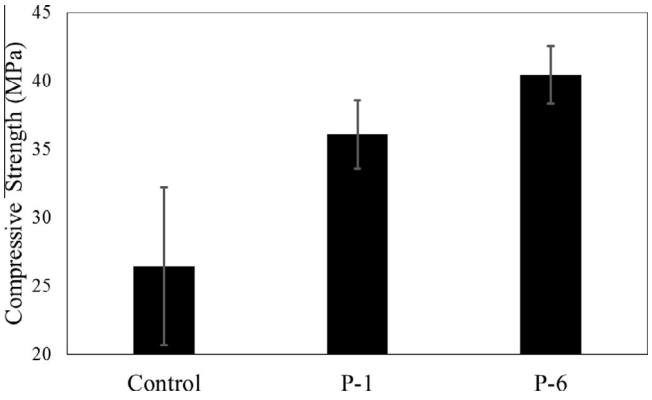

Fig. 9. Compressive strength test result of mortar samples with CNT/cement composite block at 24 h.

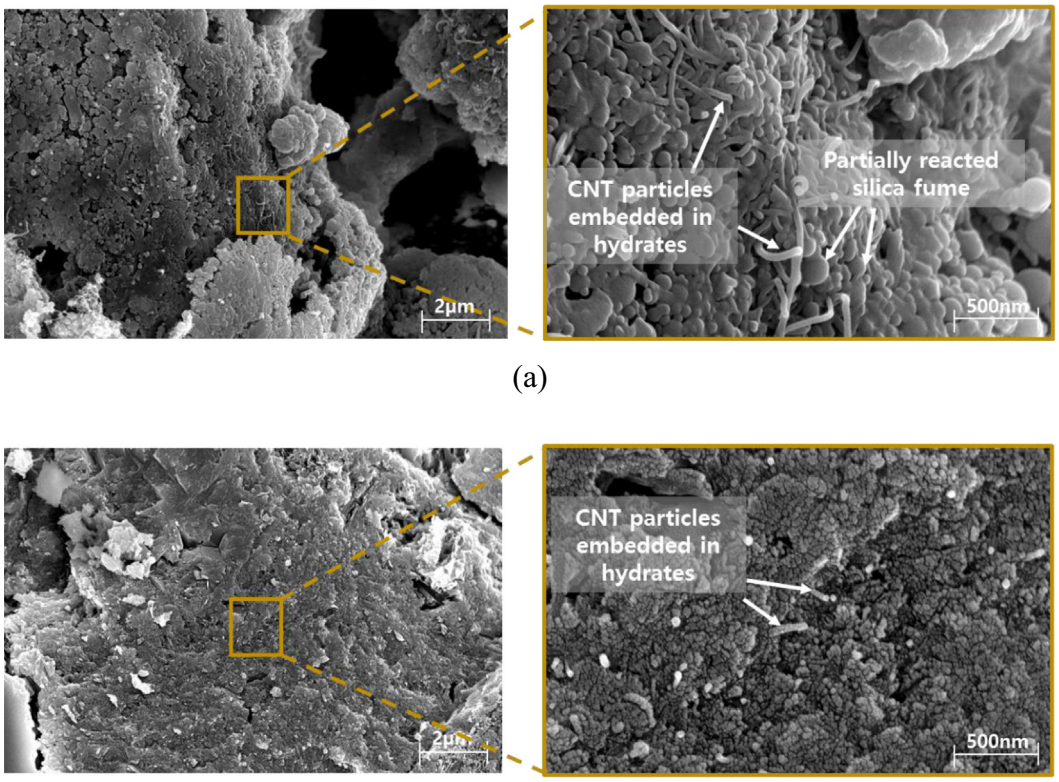

Fig. 7. SEM images of the composite block: (a) without the proposed curing and (b) with the proposed curing.

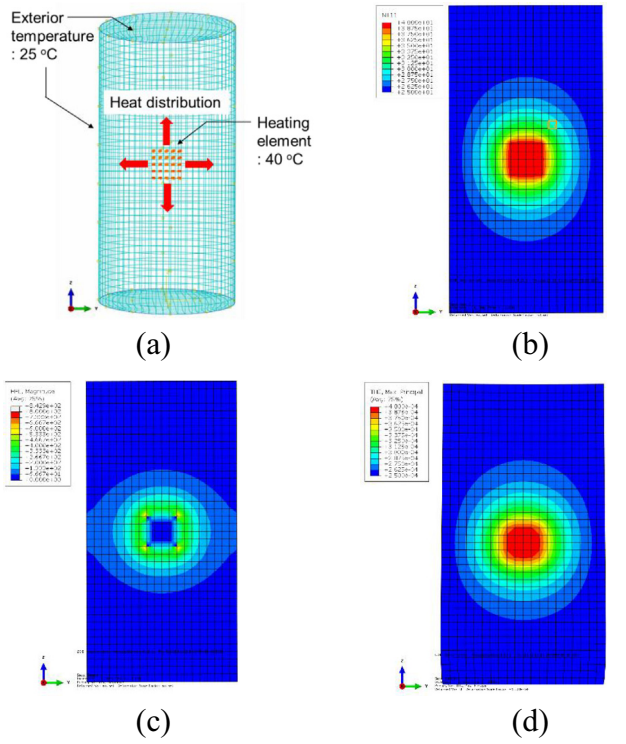

Fig. 10. (a) FE modeling for thermal analysis of the present curing method and the representative half-cut contour plots of (b) temperature distribution, (c) heat flux, and (d) thermal strain.

Note that the sample was uninsulated for thermal image analysis; thus, the temperature increase was less than the increases noted for the insulated and electrically cured samples.

Fig. 6 shows the fractional change in the electrical resistance of HP-1 and HP-6, which were composite block placed in P-1 and P-6, respectively. In the present study, the electrical resistance of the composite block increased by 1000% after heating. This increase far exceeds that observed in a previous study conducted by the present authors [23]. Meanwhile, such an increase in the electrical resistance was presumptively attributed to the pore solution of the mortar infiltrating into the composite block during the proposed curing process. Fig. 7 shows the change in the microstructure of the composite block induced by the proposed curing. In Fig. 7(a), CNT particles were shown to be effectively dispersed in hydrates and partially unreacted silica fumes were observed. In contrast, partially unreacted silica fumes were not observed in Fig. 7(b), indicating the occurrence of further hydration during the proposed curing. The additional hydration possibly occurred by the unhydrated materials in the composite as well as the reactive components in the pore solution of mortar which filtrated into the composite. The additional hydration possibly interrupted the continuity of the electrical conductive pathway that had already formed in the composite block [7,31]. The electrical resistance increase in HP-6 during the heating period was more sudden and larger than that in HP-1. It is probably attributed that a part of the input power supplied to P-1 was consumed to evaporate the free water, occurring an endothermic reaction [8]. That is, the hydration degree of the infiltrated pore solution may have been lower in P-1 than in P-6 [8]. The evaporation of free water was also

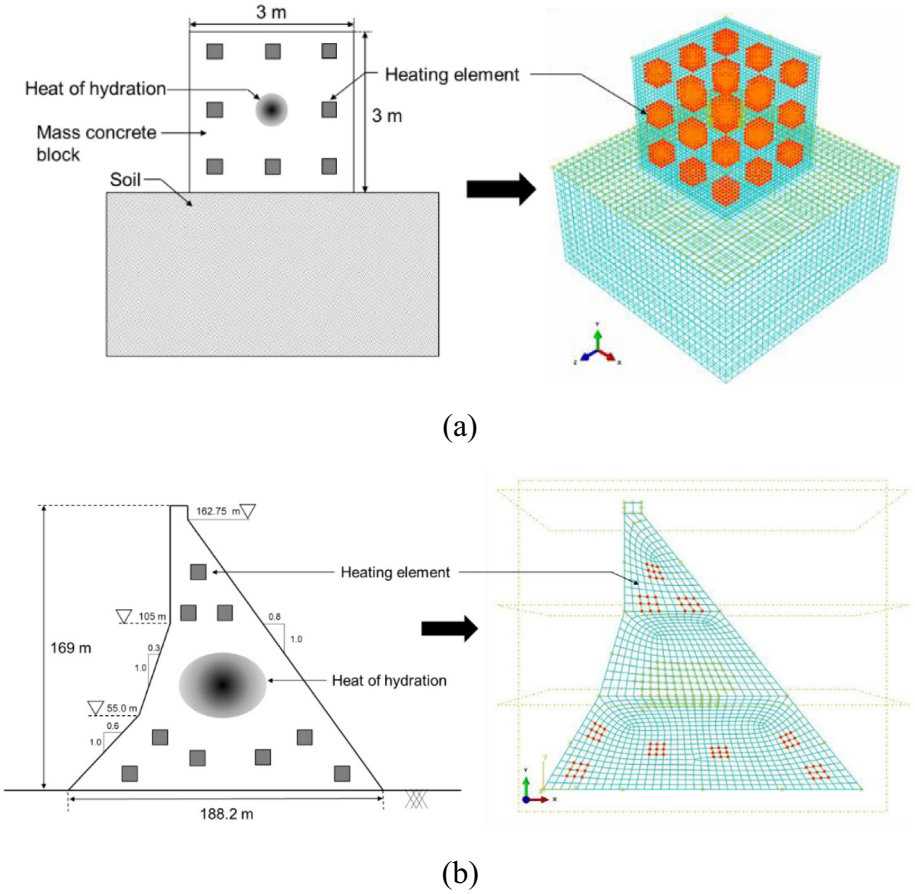

Fig. 11. Geometry and associated FE modeling of numerical examples: (a) mass concrete block [10] and (b) RCC dam [22].

responsible for the lower temperature and shorter isothermal period of P-1 in comparison with those of P-6 [8].

The designated input power and the recorded input power applied to the composite blocks are shown in Fig. 8. The designated input power was to start with 4 W, to increase to 7 W in 1.5 h, and to maintain it thereafter. The heating rate was fixed at 6.0 °C/h in this study by gradually increasing the input power as a rapid increase in the temperature may induce excessive thermal expansion in the cementitious matrix [43,9]. Previous studies recommended a heating rate lower than 20 °C/h during the heating period [9,43]. The input power applied to HP-1 and HP-6 was designed to remain at 7 W; therefore, the isothermal period was retained. Nonetheless, the input power of HP-1 and HP-6 after 10 h gradually decreased. This was due mainly to the input voltage capacity of the DC power supply which was limited at 30 V and the drastic increase in the electrical resistance of the composite block. That is, the increase in the electrical resistance of composite block lead to reduction in the current passing through it and the input voltage control was unable from that point onward. This resulted in a decrease in the temperature of P-1 and P-6 after 12.5 h.

3.3. Mechanical properties of the cylindrical specimen with composite block

The compressive strength of cement mortar samples with the proposed curing for 24 h is shown in Fig. 9. The test result showed that the compressive strength of the sample with a setting period of 6 h (P-6) was the highest. The compressive strength of P-6 increased more than 40% compared to that of normally cured sample. The compressive strength of P-1 was slightly lower than that of P-6. It is reported in previous studies that electrically cured cementitious materials exhibit the most outstanding strength when the setting period is 4–6 h [9,43]. This is due to the fact that electrical curing carried out earlier than 4–6 h can result in a thermal expansion which damages the cementitious matrix [21]. Heritage [21] reported that the thermal expansion coefficients of water, air, aggregate and cement paste in a mortar at a fresh state are all significantly different. Therefore, differential thermal expansion in the materials occurs when the mortar is heated, increasing the porosity of the mixture and reducing the strength [21]. This phenomenon elucidates why the compressive strength of P-1 was lower than that of P-6; the matrix of P-1 was damaged by the differential thermal expansion of the materials.

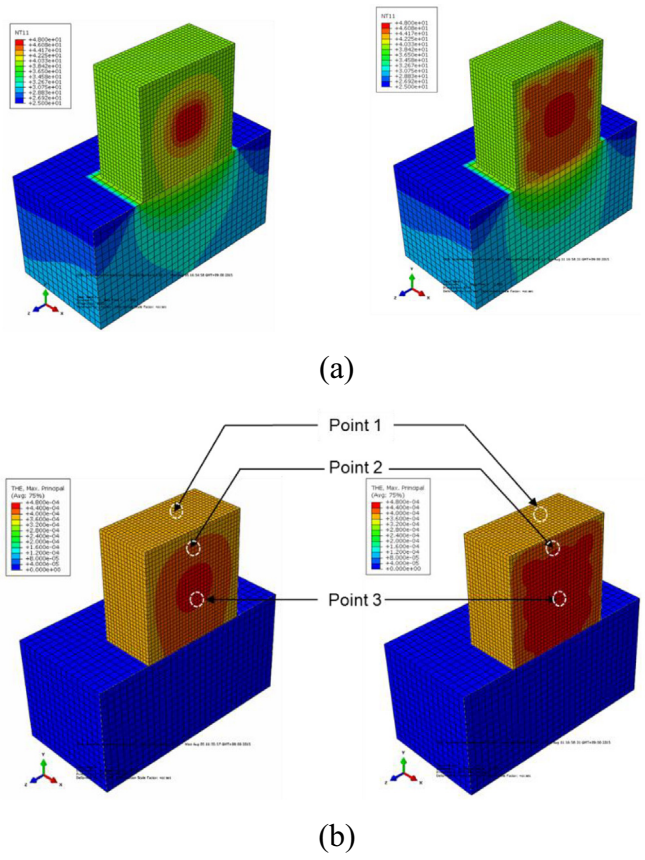

Fig. 12. FE simulation results to illustrate the effectivity of the proposed curing method on the mass concrete [10]: (a) the representative temperature distributions and (b) the predicted thermal strain.

4. Reduction of thermal crack with CNT/cement composite block: numerical analysis

Construction structures have become higher and larger in recent years, and the application scopes of a massive hardening concrete have, therefore, been a tendency to increase [38,3]. Despite the global economic crisis, megastructures have various potential benefits including economic, social and space advantages [32]. Therefore, the applicability of mass concrete is also expected to increase in the future [2]. However, higher heat of hydration, which leads to thermal cracking, is inevitably generated in mass concretes at an early age [16].

In consideration of the present curing mechanism, it is believed that the proposed curing method can be applied not only to accelerate curing but also to reduce thermal cracks in mass concretes. In this section, therefore, a FE-based thermal analysis is conducted to evaluate the potential for the application of the proposed method. Based on the experimentally obtained material constants, a series of thermal analysis of mitigation level of thermal crack in concrete were carried out. First, the previously conducted experimental conditions are reproduced in the FE model, and the relevant material and model constants are then estimated by comparing the test and simulation results.

Fig. 10(a) shows the three-dimensional FE model of the cement mortar sample with the embedded composite block. To ensure a simulation environment similar to the experimental environment, the sample size and the composite block location were identical to those in the experiment. The temperature levels of the ambient air and the composite block are set to 25 and 40 °C, respectively. The simulation results are shown in Fig. 10(b)–(d). The temperature distribution and the heat flux are predicted similarly to the experimental results as measured by a thermo-graphic camera and a temperature sensor, respectively. Here, the material coefficients of the thermal conductivity (k = 0.52 W/m) and the thermal expansion ($\alpha = 10^{-5}$) are determined through comparisons between the simulation and experimental data, which are not quite different from those in the literatures [29,18,44,35,48]. Based on the simple comparative study, the applicability potential of the proposed technique on a larger scale is numerically investigated.

By applying the abovementioned material constants, thermal analyses of two different cases are carried out, as shown in Fig. 11. Here, a simple mass concrete block [10] and a roller-compacted concrete (RCC) dams from Jaafar et al. [22] are considered in this study. FE simulation results to illustrate the effectiveness of the proposed curing method on mass concrete are shown in Figs. 12 and 13. The representative temperature distributions and the predicted thermal strain of the simple mass concrete block are exhibited in Fig. 12(a) and (b), respectively. It was found that the proposed method leads to a uniform distribution of the temperature in the concrete block, which reduces the temperature difference among the points (See, Fig. 13(b)). In addition, it is

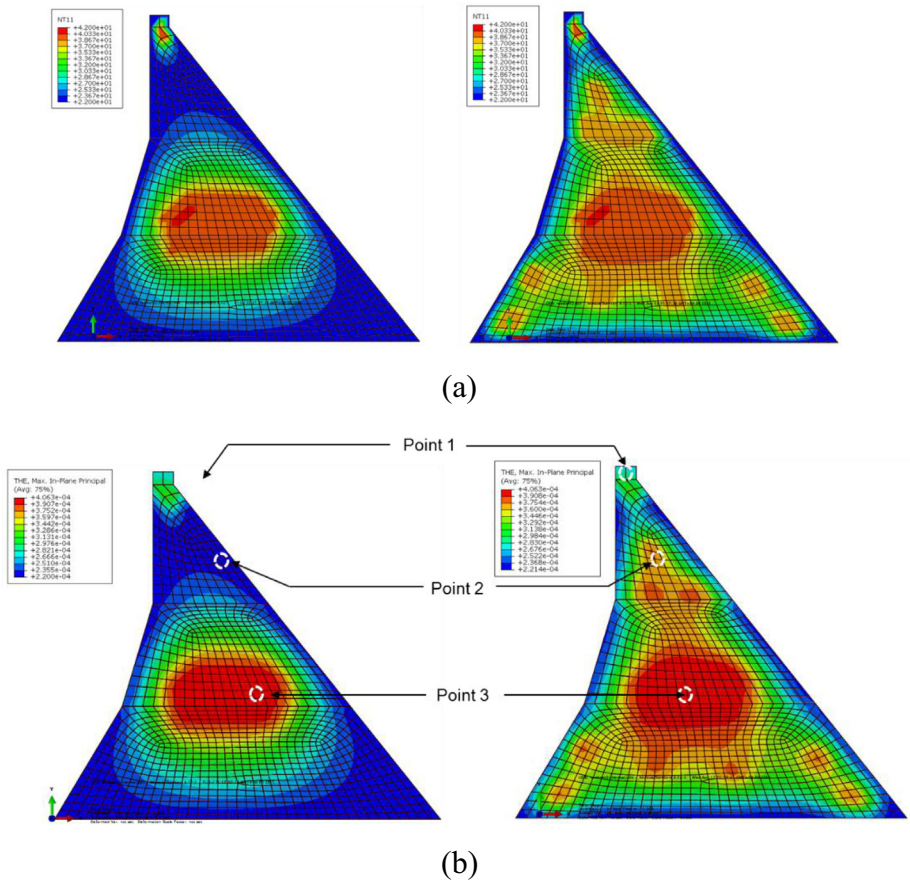

Fig. 13. FE simulation results to illustrate the effectivity of the proposed curing method on the mass concrete [10]: (a) the representative temperature distributions and (b) the predicted thermal strain.

calculated that the generated thermal expansions uniformly occurred in the mass concrete.

Fig. 13(a) and (b) present the effects of the proposed curing method on the thermal characteristics of the RCC dam. Similar to the previous thermal analysis, more evenly distributed temperature and thermal expansion results by the embedded composite blocks result from the simulation. Furthermore, Tables 4 and 5 exhibit that the calculated thermal expansion values of the concrete structures in accordance with different exterior ambient and composite block temperatures. In the Tables, it is found that the temperature differences between ambient air and the heat of hydration decreased with the application of the present technique, and the amount of thermal expansion differences is also gradually reduced. The thermal strain gap ($\Delta\varepsilon$_T) that causes the thermal cracking of concrete was shown to be significantly reduced by applying the proposed curing method, as shown in Tables 4 and 5.

The thermal cracking in concrete is generally known to mainly occur due to the heat of hydration [15], and the extent of cracks are severely elevated when the difference in the temperature between interior and exterior of concrete increases [35]. The difference in the temperature induces an inhomogeneous thermal expansion of concrete, ultimately causing the thermal cracking. Hence, minimization of the difference in the temperature within the concrete is one of possible solution for the thermal cracking reduction [38]. In accordance with the previous studies [38,15,35], it is also known that the thermal strain gap ($\Delta\varepsilon$T) is the constant which can be directly associated with the thermal cracking. The calculation results of the present thermal analysis suggest that the proper

Table 4
Simulation results of the FE-based thermal analysis (simple mass concrete).

Hydration heat (Point 3, °C)	Temperature of the composite block (°C)	Exterior temperature (Point 1, °C)	Thermal strain gap ($\Delta\varepsilon_T$) (Δ Point 2 – Point 3, $\times 10^{-4}$)
48	30	0	2.22
		25	1.87
		40	1.66
	40	0	1.37
		25	1.01
		40	0.80
	50	0	0.51
		25	0.16
		40	0.06

Table 5
Simulation results of the FE-based thermal analysis (RCC dam).

Hydration heat (Point 3, °C)	Temperature of the composite block (°C)	Exterior temperature (Point 1, °C)	Thermal strain gap ($\Delta\varepsilon_T$) (Δ Point 2 – Point 3, $\times 10^{-4}$)
42	30	0	1.14
		25	1.02
		40	0.95
	40	0	0.19
		25	0.07
		40	0.01
	50	0	0.88
		25	0.76
		40	0.01

utilization of the proposed curing method could contribute to diminish the damage caused by thermal cracking.

Overall, the proposed method for accelerated curing has the following advantages compared to the previous curing methods such as stream, microwave and electrical curing methods: 1) the uniform heat conduction can be ensured through adjusting the location of composite block, 2) the heat loss can be minimized since the heat generation is initiated from internal point of cementitious materials and 3) the input power needed to the proposed curing method is lower than that of the previous electrical curing method.

5. Concluding remarks

The present study investigated an accelerated curing method of cement mortar with electrically conductive CNT/cement composite block. An electrically conductive CNT/cement composite block was placed in the middle of cement mortar samples and input voltages were applied to the composite. The obtained result in this study indicates that the electrically conductive CNT/cement composite block is applicable to the cement mortar curing and reduction of thermal cracking of massive concretes structures. The main findings of the present study can be summarized as follows:

(1) The heating rate of the composite block embedded into the cement mortar sample was fixed at 6.0 °C/h in this study by gradually increasing the input power from 4 W to 7 W. The surface temperature of the cement mortar sample increased by approximately 50 °C in the isothermal period and was maintained at this level until 12.5 h.
(2) The electrical resistance of the composite blocks in the cement mortar sample increased by 1000% after the proposed curing process. The electrical resistance increase of the composite block placed in the cement mortar sample with a setting period for 6 h was more sudden and larger than the embedded into the cement mortar sample with a setting period for 1 h.
(3) The compressive strength of the cement mortar sample with a setting period of 6 h was highest. The compressive strength of the sample increased more than 40% compared to that of normally cured sample.
(4) In the finite element simulation, the proposed method leads to a uniform distribution of the temperature in the concrete block, which reduces the temperature difference among the points. As a result, the expansion difference is also gradually reduced.

It can be concluded that the proposed curing method is an effective means of accelerating the curing of concrete and decreasing the occurrence probability of thermal cracks in massive concretes. A further study is needed to investigate the effect of the proposed curing method on the working strength of cementitious materials, associated with the mechanical properties in a service condition.

Acknowledgements

This research was supported by a grant (15CTAP-C098086-01) from Technology Advancement Research Program (TARP) Program funded by Ministry of Land, Infrastructure and Transport of Korean government.

Appendix A. Supplementary data

Supplementary data associated with this article can be found, in the online version, at http://dx.doi.org/10.1016/j.compstruct.2016.09.014.

References

[1] Al-Khaiat H, Haque MN. Effect of initial curing on early strength and physical properties of a lightweight concrete. Cem Concr Res 1998;28(6):859–66.
[2] Al-Kodmany K. Tall buildings, design, and technology: visions for the twenty-first century city. J Urban Technol 2011;18(3):115–40.
[3] Ali MM, Moon KS. Structural developments in tall buildings: current trends and future prospects. Archit Sci Rev 2007;50(3):205–23.
[4] American Society for Testing and Materials, ASTM C39. Standard test method for compressive strength of cylindrical concrete specimens. West Conshohocken, PA: ASTM International; 2012.
[5] Athanasopoulos N, Sikoutris D, Panidis T, Kostopoulos V. Numerical investigation and experimental verification of the Joule heating effect of polyacrylonitrile-based carbon fiber tows under high vacuum conditions. J Compos Mater 2011. 0021998311430159.
[6] Azhari F, Banthia N. Cement-based sensors with carbon fibers and carbon nanotubes for piezoresistive sensing. Cement Concr Compos 2012;34(7):866–73.
[7] Bakharev T, Sanjayan JG, Cheng Y-B. Resistance of alkali-activated slag concrete to carbonation. Cem Concr Res 2001;31(9):1277–83.
[8] Barreira E, de Freitas VP. Evaluation of building materials using infrared thermography. Constr Build Mater 2007;21(1):218–24.
[9] Bredenkamp S, Kruger K, Bredenkamp GL. Direct electric curing of concrete. Mag Concr Res 1993;45(162):71–4.
[10] Buffo-Lacarrière L, Sellier A, Escadeillas G, Turatsinze A. Multiphasic finite element modeling of concrete hydration. Cem Concr Res 2007;37(2):131–8.
[12] Chang JJ, Yeih W, Huang R. Degradation of the bond strength between rebar and concrete due to the impressed cathodic current. J Mar Sci Technol 1999;7(2):89–93.
[13] Costa P, Silva J, Ansón-Casaos A, Martinez MT, Abad MJ, Viana J, et al. Effect of carbon nanotube type and functionalization on the electrical, thermal, mechanical and electromechanical properties of carbon nanotube/styrene–butadiene–styrene composites for large strain sensor applications. Compos B Eng 2014;61:136–46.
[14] Park JM, Kim PG, Jang JH, Wang Z, Kim JW, Lee WI, et al. Self-sensing and dispersive evaluation of single carbon fiber/carbon nanotube (CNT)-epoxy composites using electro-micromechanical technique and nondestructive acoustic emission. Compos B Eng 2008;39(7):1170–82.
[15] De Schutter G. Finite element simulation of thermal cracking in massive hardening concrete elements using degree of hydration based material laws. Comput Struct 2002;80(27):2035–42.
[16] Emborg M, Bernander S. Assessment of risk of thermal cracking in hardening concrete. J Struct Eng 1994;120(10):2893–912.
[17] Erdem TK, Turanli L, Erdogan TY. Setting time: an important criterion to determine the length of the delay period before steam curing of concrete. Cem Concr Res 2003;33(5):741–5.
[18] Fu X, Chung DDL. Effect of admixtures on thermal and thermo-mechanical behavior of cement paste. ACI Mater J 1999;96(4):455–61.
[19] Han B, Yu X, Ou J. Effect of water content on the piezoresistivity of MWNT/cement composites. J Mater Sci 2010;45(14):3714–9.
[21] Heritage I. Direct electric curing of mortar and concrete [Doctoral dissertation]. Edinburgh Napier University; 2001.
[22] Jaafar MS, Bayagoob KH, Noorzaei J, Thanoon WA. Development of finite element computer code for thermal analysis of roller compacted concrete dams. Adv Eng Softw 2007;38(11):886–95.
[23] Kim GM, Naeem F, Kim HK, Lee HK. Heating and heat-dependent mechanical characteristics of CNT-embedded cementitious composites. Compos Struct 2016;136:162–70.
[24] Kim HK, Nam IW, Lee HK. Enhanced effect of carbon nanotube on mechanical and electrical properties of cement composites by incorporation of silica fume. Compos Struct 2014;107:60–9.
[25] Kim JK, Moon YH, Eo SH. Compressive strength development of concrete with different curing time and temperature. Cem Concr Res 1998;28(12):1761–73.
[26] Lerner L. Physics for scientists and engineers. Jones & Bartlett; 1997. pp. 732–733.
[27] Leung CK, Pheeraphan T. Microwave curing of Portland cement concrete: experimental results and feasibility for practical applications. Constr Build Mater 1995;9(2):67–73.
[28] Liu CC, Lee C, Wang WC. Study of autoclave methods for evaluating the alkali-silica reactivity of aggregates. J Chin Inst Eng 2011;34(5):663–70.
[29] Meyers SL. Thermal coefficient of expansion of Portland cement-long-time tests. Ind Eng Chem 1940;32(8):1107–12.
[30] Nurse RW. Steam curing of concrete. Mag Concr Res 1949;1(2):79–88.
[31] Parra-Montesinos GJ, Garrecht H. High performance fiber reinforced cement composites 6. RILEM 2012:102–5.
[32] Qian Z. Building Hangzhou's new city center: mega project development and entrepreneurial urban governance in China. Asian Geogr 2011;28(1):3–19.
[33] Reza F, Yamamuro JA, Batson GB. Electrical resistance change in compact tension specimens of carbon fiber cement composites. Cement Concr Compos 2014;26:873–81.
[34] Saul AGA. Principles underlying the steam curing of concrete at atmospheric pressure. Mag Concr Res 1951;2(6):127–40.

[35] Sellevold EJ, Bjøntegaard Ø. Coefficient of thermal expansion of cement paste and concrete: mechanisms of moisture interaction. Mater Struct 2006;39(9):809–15.
[36] Souri H, Nam IW, Lee HK. A zinc oxide/polyurethane-based generator composite as a self-powered sensor for traffic flow monitoring. Compos Struct 2015;134:579–86.
[37] Souri H, Nam IW, Lee HK. Electrical properties and piezoresistive evaluation of polyurethane-based composites with carbon nano-materials. Compos Sci Technol 2015;121:41–8.
[38] Springenschmid R. Prevention of thermal cracking in concrete at early ages, vol. 15. CRC Press; 1998.
[39] Tuan CY, Yehia S. Evaluation of electrically conductive concrete containing carbon products for deicing. ACI Mater J 2004;101(4).
[40] Tyson BM, Al-Rub RKA, Yazdanbakhsh A, Grasley Z. A quantitative method for analyzing the dispersion and agglomeration of nano-particles in composite materials. Compos B Eng 2011;42(6):1395–403.
[41] Vaidya S, Allouche EN. Strain sensing of carbon fiber reinforced geopolymer concrete. Mater Struct 2011;44:1467–75.
[42] Wang S, Wen S, Chung DDL. Resistance heating using electrically conductive cements. Adv Cem Res 2004;16(4):161–6.
[43] Wilson JG, Gupta NK. Equipment for the investigation of the accelerated curing of concrete using direct electrical conduction. Measurement 2004;35(3):243–50.
[44] Xu Y, Chung DDL. Improving silica fume cement by using silane. Cem Concr Res 2000;30(8):1305–11.
[45] Xuenquan W, Jianbgo D, Mingshu T. Microwave curing technique in concrete manufacture. Cem Concr Res 1987;17(2):205–10.
[46] Yang BJ, Cho KJ, Kim GM, Lee HK. Effect of CNT agglomeration on the electrical conductivity and percolation threshold of nanocomposites: a micromechanics-based approach. CMES Comput Model Eng Sci 2014;103(5):343–65.
[47] Yang BJ, Souri H, Kim S, Ryu S, Lee HK. An analytical model to predict curvature effects of the carbon nanotube on the overall behavior of nanocomposites. J Appl Phys 2014;116(3):033511.
[48] Yang BJ, Na S, Jang JG, Kim HK, Lee HK. Thermo-mechanical analysis of road structures used in the on-line electric vehicle system. Struct Eng Mech 2015;53(3):519–36.
[49] Yu X, Kwon E. A carbon nanotube/cement composite with piezoresistive properties. Smart Mater Struct 2011;18(5):1–5.